Iraqi Journal of Information and Communications Technology(IJICT)
Conference Series: The 1st Conference of Applied Researches in Information Engineering(ARIE2021), 2021

ISSN:2222-758X
e-ISSN:2789-7362

DESIGN OF OPTIMAL INVERSE KINEMATIC SOLUTION FOR HUMANOID ROBOTIC ARMS

Saif F. Abulhail [1], Mohammed Z. Al-Faiz [2]
[1,2] College of Information Engineering, Al-Nahrain University, Baghdad, Iraq
{saifabulhail80, mzalfaiz12}@gmail.com [1,2]
Received:6/5/2021, Accepted:19/6/2021

***Abstract*- One of the main problems in robotics is the Inverse Kinematics (IK) problem. In this paper, three optimization algorithms are proposed to solve the IK of Humanoid Robotic Arms (HRAs). A Particle Swarm Optimization (PSO), Social Spider Optimization (SSO), and Black Hole Optimization (BHO) algorithms are proposed to optimize the parameters of the proposed IK. Each optimization method is applied on both arms to find the desired positions and required angles with a minimum error. Denavit-Hartenberg (D-H) method is used to design the model of HRAs for both arms in which each arm has five Degree Of Freedom (DOF). The HRAs model is tested for performance by several positions to be reached by both arms at the same time to find which optimization algorithm is better. Optimal solutions obtained by SSO, PSO and BHO algorithms are evaluated and listed in a comparison table between them. These optimization algorithms are assessed by calculating the Computational Time (CT) and Root Mean Squared Error (RMSE) for the absolute error vector of the positions. Calculation and simulation results showed that BHO is better than PSO and SSO algorithms from point of view of CT and RMSE. The worst RMSE is 0.0864 was calculated using the PSO algorithm. But longer CT is 7.6521 seconds, which was calculated using SSO. While the best RMSE and shorter CT.are 2×10^{-7} and 3.0156 seconds respectively were calculated by BHO. Moreover, in this paper, the Graphical User Interface (GUI) is designed for motional characteristics of the HRAs model in the Forward Kinematics (FK) and IK.**

keywords: **Denavit-hartenberg, Black hole optimization, Humanoid robotic arms, Inverse kinematics, Graphical user interface, Social spider optimization.**

I. INTRODUCTION

IK solution is significant for humanoid robot interactions, particularly for applications like teaching a robot to execute a series of coordinated gestures or telesurgery applications. There are many parts to controlling a robotic manipulator. The major parts are the FK and IK of the arm links. The position and orientation are computed by the FK of the HRAs model depending on the joint's angle. The IK is used to compute the arm's angles based on specified position and orientation. The IK solution is provided by many methods like iterative, geometrical solutions, numerical and algebraic [1] . Nature-inspired metaheuristic algorithms are suitable for solving IK. A wide-ranging nature algorithm has been presented over the last twenty years. For example, ant colony, genetic algorithm and PSO. The ant colony optimization is motivated by the activities of ant's colonies, which are capable to obtain the optimal path (smallest path) to the food. A genetic algorithm also is a search and optimization technique based on genetic nature. PSO was motivated by the swarm actions [2] . The main concept of any method is to model the arm as series of joints and allocate a reference joint to begin the movement. D-H method is one of the main methods that are used in the modeling of robotic arms joints. The arm movement is transformed for all links and all the transformations are obtainable in the transformation matrix [3] . The IK proposed in [4] based on a brain-computer interface is designed to extract and analyse Electroencephalogram signals. The IK of the extracted signal is evaluated on the expected position to make the arm be reached to the desired position. In that work, the researchers used only one arm which is the right arm, they did not take into consideration the high accuracy of the

ISSN:2222-758X
e-ISSN:2789-7362

arm in reaching the desired position. Also, they did not apply any optimization method to the IK, and therefore there is a percentage of error in the accuracy of the arm. The analytical solution proposed in [5] is based on the D-H method to find the solution of an IK problem and obtain a mathematical model 6-DOF robotic arm. The researchers in [6] presented PSO to optimize PID controller parameters and they used the PSO algorithm to control the human arm. The model proposed in [7] found the performance of PSO when used to solve IK. In that model, the optimization algorithm was used for a double link articulated system. The researchers in [8] proposed a proportional integral derivative controller for controlling a class of nonlinear robotic manipulators. The parameters of the designed controller are obtained based on the BHO algorithm. The researchers in [9] suggested a BHO algorithm to improve the clustering result. They tested six datasets using the BHO algorithm. They showed that the proposed algorithm clustered the data items efficiently. The researchers in [10] presented the BHO algorithm to optimize the parameter of the nonlinear controller. They showed the efficiency of that optimization algorithm and nonlinear controller for solving different problems of nonlinear models. In this paper, three optimization algorithms are proposed to obtain an IK solution for both arms to reach the desired position by determining the optimal angles of the HRAs model with a minimum error. Each optimization method is applied on both arms simultaneously. The main contribution of this paper is to reach the end effector of each arm with higher accuracy to control both arms at the same time and found which optimization technique has a minimum error and less CT which is the length of time required to perform a computational optimization algorithm. The rest of this paper is organized as follows: In Section II, the proposed model is described. A brief explanation of the BHO, SSO and PSO for solving IK is given in Section III. Section IV illustrates the limitations and scenarios of the HRAs model. In section V, the results of the HRAs model is evaluated and discussed by calculating the CT and RMSE for the absolute error vector of the reference position. Moreover, in this section, GUI is designed for the HRAs model to simulate the movement of the HRAs model to reach the desired position. Finally, section VI includes the conclusion of this work.

II. PROPOSED HRAS MODEL

The kinematic chain of the HRAs was defined based on the Denativ-Hartenberg (D-H) technique where the direction of joints rotation is around the z-axis. The displacement between two joints is called the common normal and represents the x-axis. The kinematic scheme of the constructed 5-DOF HRAs with its system of the axis is showed in Fig. 1. The D-H parameter corresponding to the configuration of the link is presented in Table I.

TABLE I
D-H Parameters of HRAs Model

Joint number	Right arm				Left arm			
	d_i	$\propto_i$	q_i	a_i	d_j	$\propto_j$	q_j	a_j
1	0	$\frac{\pi}{2}$	$q_{1r}+\frac{\pi}{2}$	0	0	$\frac{\pi}{2}$	$q_{1l}+\frac{\pi}{2}$	0
2	0	$\frac{-\pi}{2}$	$q_{2r}+\frac{\pi}{2}$	0	0	$\frac{\pi}{2}$	$q_{2l}+\frac{\pi}{2}$	0
3	0	0	q_{3r}	L1	0	0	q_3l	L1
4	0	$\frac{-\pi}{2}$	$q_{4r}+\frac{\pi}{2}$	0	0	$\frac{-\pi}{2}$	q_4l	0
5	L2	0	q_5r	0	L2	0	q_5l	0

Where the representation of the angle's rotation about Z is q, the symbol of the displacement along the z-axis is d , the rotation about the x-axis is denoted as $\propto_i$. The length of L1 and L2 is (35) cm and (29) cm respectively. These parameters

ISSN:2222-758X
e-ISSN:2789-7362

are used to describe the orientation and position for both arms by transformation matrices that are representing the FK matrices and they can be denoted by the following equations:

$$A_i = \begin{bmatrix} cos\, qi & -cos\ \propto_i \times sin\, q_i & sin \propto_i \times sin\, q_i & a_i \times cos\, q_i \\ sin\, q_i & cos \propto_i \times cos\, q_i & -cos\, q_i \times sin\ \propto_i & a_i \times sin\, q_i \\ 0 & sin \propto_i & cos \propto_i & d_i \\ 0 & 0 & 0 & 1 \end{bmatrix} \tag{1}$$

$$A_{1R} = \begin{bmatrix} -S_1 & 0 & C_1 & 0 \\ C_1 & 0 & S_1 & 0 \\ 0 & 1 & 0 & 0 \\ 0 & 0 & 0 & 1 \end{bmatrix} \tag{2}$$

$$A_{2R} = \begin{bmatrix} -S_2 & 0 & -C_2 & 0 \\ C_2 & 0 & -S_2 & 0 \\ 0 & -1 & 0 & 0 \\ 0 & 0 & 0 & 1 \end{bmatrix} \tag{3}$$

$$A_{3R} = \begin{bmatrix} C_3 & -S_3 & 0 & L_1 * C_3 \\ S_3 & C_3 & 0 & L_1 * S_3 \\ 0 & 0 & 1 & 0 \\ 0 & 0 & 0 & 1 \end{bmatrix} \tag{4}$$

$$A_{4R} = \begin{bmatrix} -S_4 & 0 & -C_4 & 0 \\ C_4 & 0 & -S_4 & 0 \\ 0 & -1 & 0 & 0 \\ 0 & 0 & 0 & 1 \end{bmatrix} \tag{5}$$

$$A_{5R} = \begin{bmatrix} C_5 & -S_5 & 0 & 0 \\ S_5 & C_5 & 0 & 0 \\ 0 & 0 & 1 & L_2 \\ 0 & 0 & 0 & 1 \end{bmatrix} \tag{6}$$

where, (i=1R,2R,...,5R) for the right and notice that, $cos(q)$ is denoted by C and $sin(q)$ is denoted by S.

$$T_{5R}^{1R} = A_{1R} \times A_{2R} \times A_{3R} \times A_{4R} \times A_{5R} = \begin{bmatrix} rn_x & ro_x & ra_x & r_x \\ rn_y & ro_y & ra_y & r_y \\ rn_z & ro_z & ra_z & r_z \\ 0 & 0 & 0 & 1 \end{bmatrix} \tag{7}$$

ISSN:2222-758X
e-ISSN:2789-7362

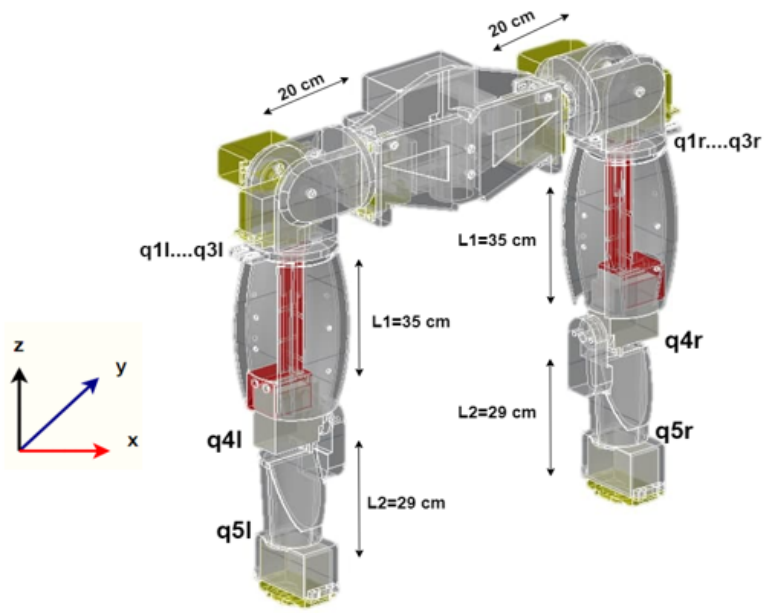

Figure 1: Kinematic model of HRAs

In Eq. 7, the FK of the right arm is solved in which $r_x r_y r_z$ are the position parameters, rn_x, rn_y, rn_z, ro_x, ro_y, ro_z, ra_x, ra_y and ra_z are right rotation variables. The whole matrix of the end effector of the right arm is represented by T_{5R}^{1R}. The FK of the left arm is determined in the same way that the right arm obtained but the D-H parameters for the left arm is used like the following equation.

$$T_{5L}^{1L} = A_{1L} \times A_{2L} \times A_{3L} \times A_{4L} \times A_{5L} = \begin{bmatrix} ln_x & lo_x & la_x & l_x \\ ln_y & lo_y & la_y & l_y \\ ln_z & lo_z & la_z & l_z \\ 0 & 0 & 0 & 1 \end{bmatrix} \tag{8}$$

Where, l_x, l_y and l_z are the left position parameters and the left rotation parameters are ln_x, ln_y, ln_z, lo_x, lo_y, lo_z, la_x, la_y and la_z . The whole matrix of the end effector of the left arm is represented by T_{5L}^{1L} as the whole matrix.

III. Solution of Inverse Kinematic

A. BHO Algorithm

The BHO is an algorithm depending on the population. It has many mutual features with other population-based methods. It is created to analyzing clustering data that is used for optimizing and tuning parameters. The concept of the black hole (BH) occurrence is that a BH in space has an enormous concentration. mass. In BH, there are no choices for objects to take away from their gravity. Everything that falls inside the BH, including light particles, can vanish from our universe. The primary population of candidate solutions is starting then an optimization problem is defined to calculate the fitness function calculated for them. In these algorithms, the best candidate will be chosen in each iteration to be a BH and after

ISSN:2222-758X
e-ISSN:2789-7362

that, the rest of the stars will make up the regular stars. The BH starts gulping stars neighboring it after the initialization process. In this situation, a new candidate (star) is arbitrarily created in the search space. The sphere that represents the limitation boundary of the BH in-universe is recognized as the Event Horizon (EH). The radius of the EH is named the Schwarzschild radius. The escape speed is equivalent to the speed of light, at this radius. The Schwarzschild radius in the BHO is described by the following equation [11]:

$$r = \frac{2gm}{c^2} \tag{9}$$

Where the gravitational constant is represented by g , the mass of the BH is represented by m and the speed of light is represented by c. The BH algorithm starts with the initialization of population (P) that is randomly generate the star solution (candidate) and located in the search space. The BH begins swallowing the stars nearby it and the stars begin moving to the BH. The swallowing of each star is denoted as the following equation:

$$X_j(t+1) = X_j(t) + rand \times (X_{BH} - X_j(t)),\ j = 1, 2, 3....N \tag{10}$$

Where the locations of the jth star are represented by $X_j(t)$ and $X_j(t+1)$, N is the number of stars and the iteration is represented t. The location of the BH in the search space is represented by X_{BH} . The. rand is a number between $[-1, 1]$. While moving towards the BH, a star may arrive at a position with a lower cost than the BH. In such a case, the BH replaces the location with that star. For the HRAs, it's required to find the solution to the IK problem to find the 10 angles that achieve the desired position of both arms. In BHO for IK, each BH is designed to have 9 dimensions equal to the number of parameters to be optimized. These parameters are rotation parameters in Eq. 7 and Eq. 8. Each X_{BH} that represents the BH in Eq. 10 is designed to have nine locations that include right rotation matrix variables for the right arm (rn_x, rn_y, rn_z, ro_x, ro_y, ro_z, ra_x, ra_y and ra_z) and left rotation matrix parameters ln_x, ln_y, ln_z, lo_x, lo_y, lo_z, la_x, la_y and la_z. In IK, the precise calculations of q values are main significant. The wrist angle value (q_{5r} and q_{5l}) are assumed always equal to zero because it represents the end effector of the HRAs model and therefore does not affect the position of the HRAs model. Using the matrix parameters provided in Eq. 7 and Eq. 8 and the D-H parameters in Table I, the solutions of the optimal joint angles for both arms are given directly as follows:

$$q_{1r} = tan^{-1}(\frac{-ro_y}{ro_x}) \tag{11}$$

$$q_{2r} = tan^{-1}(\frac{r_x S_1 + r_y C_1}{r_z}) \tag{12}$$

$$q_{3r} = tan^{-1}(\frac{S_3}{C_3}),\ where,\ C_3 = \frac{r_z - ra_z L_2}{-L1 * C_2}\ and\ S_3 = \sqrt{1 - C_3^2} \tag{13}$$

$$q_{4r} = cos^{-1}(\frac{-rnz}{c_2} - (q_{3r})) \tag{14}$$

$$q_{1l} = tan^{-1}(\frac{lo_y}{lo_x}) \tag{15}$$

$$q_{2l} = tan^{-1}(\frac{S_2}{C_2}),\ where,\ C_2 = loz\ and\ S_2 = \sqrt{1 - C_2^2} \tag{16}$$

ISSN:2222-758X
e-ISSN:2789-7362

$$q_{3l} = tan^{-1}(\frac{S_3}{C_3}),\ where,\ C_3 = \frac{la_z \times L_{2-lz}}{L_1 \times C_2}\ and\ S_3 = \sqrt{1 - C_3^2} \tag{17}$$

$$q_{4l} = sin^{-1}(\frac{laz}{c_2} - (q_{3l})) \tag{18}$$

In BHO, the possibility of crossing the EH of BH throughout moving stars to the BH is used to assemble the optimum data from the search area. If any distance between a star and the BH is less than the radius of the EH, that star crosses the EH of the BH will be swallowed by the BH. In such cases, another star is populated and distributed randomly over the search space. The radius of the EH in the BHO is calculated by the following expression:

$$R = \frac{fitness_{BH}}{\sum_{k=1}^{N} fitness_k} \tag{19}$$

where $fitness_{BH}$ is the fitness of BH and $fitness_k$ is the fitness kth star. The number of candidates (stars solutions) is represented by N.

B. SSO Algorithm

The social spider approach is a search depending on the performance of the spiders [12]. Depending on the natural laws of the mutual colony, every person repeats a collection of spiders that connect. The algorithm has two different search agents (spiders): males and females. The choice of the female's number N_{feml} is within the range of 90%-65% of the entire society N. Thus, the formulation equation of N_{feml} is showed in Eq. 20

$$N_{feml} = [(0.9 - rand(0.1) \times 0.25) \times N] \tag{20}$$

N_{mal} is the total of the male spider. It is calculated by the following equation:

$$N_{mal} = N - N_{feml} \tag{21}$$

Each spider gets its weight w_j depending on the provided approach that presents the solution quality that is belonging to the population S and the spider j. The w_j is presented by the following equation [12]:

$$w_j = \frac{J(s) - worst_s}{best_{s-worst_s}} \tag{22}$$

Like other methods, population initializing is an iterative procedure of the SSO. In the entire population, females and males are the first initialization. After that, the initializing of the set S and the spider N locations are completed. In SSO computing for IK, the size of each spider is 9 as in BHO equivalent to the number of parameters to be optimized. Female and male spiders are showed in Eq. 23 and Eq. 24. These spiders are including the parameters to be optimized. The spider values are reliably and randomly spread between the upper bound of the original parameter p_j^{high} and lower bound of initial parameter p_j^{low} [13].

$$f_{i,j}^0 = p_j^{low} + rand \times (p_j^{high} - p_j^{low}) \tag{23}$$

$$m_{i,j}^0 = p_j^{low} + rand \times (p_j^{high} - p_j^{low}) \tag{24}$$

Where $i = 1, 2...N_{feml}$, $k = 1, 2....N_{mal}$, j=1,2....N and zero represent the initial population.

ISSN:2222-758X
e-ISSN:2789-7362

C. PSO Algorithm

One of the main benefits of the PSO algorithm is simply applied. This algorithm generates a swarm (population) of particles (candidate solutions). The optimal solution was reached by particles using their position and velocity [12]. Only two equations are updated at each iteration, velocity update as in Eq. 25 and position update as in Eq. 26.

$$vel_{it} = vel_{it} + D1 \times R_1 \times (Pers_{best} - x_{it}) + D2 \times R_2 \times (glob_{best} - x_{it}) \tag{25}$$

$$x_{it} = x_{it} + vel_{it} \tag{26}$$

Where the dimension is represented as t =1, 2, ...,9, swarm size is denoted by i, $pers_{best}$ is the personal best and $glob_{best}$ is the global best. The weight of personal is represented by D1 and D2. Random numbers are denoted as R1 and R2 distributed regularly between [-1,1]. After calculating the optimal parameters by SSO and PSO algorithms, we obtain the solution of IK for right and left angles as in BHO by Eq. 11 to Eq. 18. The choice of the fitness function is very essential. It plays the main role in finding the optimal solution of the parameters to be optimized. For three optimization algorithms, we selected RMSE as a fitness function in this paper for BHO, SSO and PSO. The positional error of the end effector is checked using the angles of both arms then calculate the RMSE of the absolute error vector between the desired and actual position as follows:

$$\begin{bmatrix} ex_r \\ ey_r \\ ez_r \end{bmatrix} = \left| \begin{bmatrix} r_x - R_x^a \\ r_y - R_y^a \\ r_z - R_z^a \end{bmatrix} \right| \tag{27}$$

$$Rfitness = \sqrt{\frac{(ex_r)^2 + (ey_r)^2 + (ez_r)^2}{3}} \tag{28}$$

$$\begin{bmatrix} ex_l \\ ey_l \\ ez_l \end{bmatrix} = \left| \begin{bmatrix} l_x - L_x^a \\ l_y - L_y^a \\ l_z - L_z^a \end{bmatrix} \right| \tag{29}$$

$$Lfitness = \sqrt{\frac{(ex_l)^2 + (ey_l)^2 + (ey_l)^2}{3}} \tag{30}$$

Where Rfitness and Lfitness are fitness values for right and left arms respectively, $[ex_r, ey_r, ez_r, ex_l, ey_l, ez_l]$ is the absolute error vector in x, y, z axis respectively, $[r_x, r_y, r_z, l_x, l_y, l_z]$ are the required position vector, and $[R_x^a, R_y^a, R_z^a, L_x^a, L_x^a, L_x^a]$ are the actual position vector for the right and left arm. The settings of BHO, SSO, and PSO parameters are listed in Table II. For three optimization algorithms, they are synthesized in m-file function using MATLAB facilities and they recall the IK many times and they are evaluating the fitness functions at every iteration. After that, the pre-optimized parameters are applied at the same time into the IK of the HRAs model to calculate the error to find the optimum solution thus optimum angles and desired position at the end of generations. Consequently, the measured error is used to obtain the fitness function and compared to the previous one at each iteration to find the optimal solution. Finally, after a certain number of iterations, this process is repeated until the optimal parameters are found. Fig. 2 describes in flowchart the procedure of how the

ISSN:2222-758X
e-ISSN:2789-7362

BHO algorithm evaluates the optimal parameters and is then used to the IK. Also, the SSO flowchart is showed in Fig. 3.

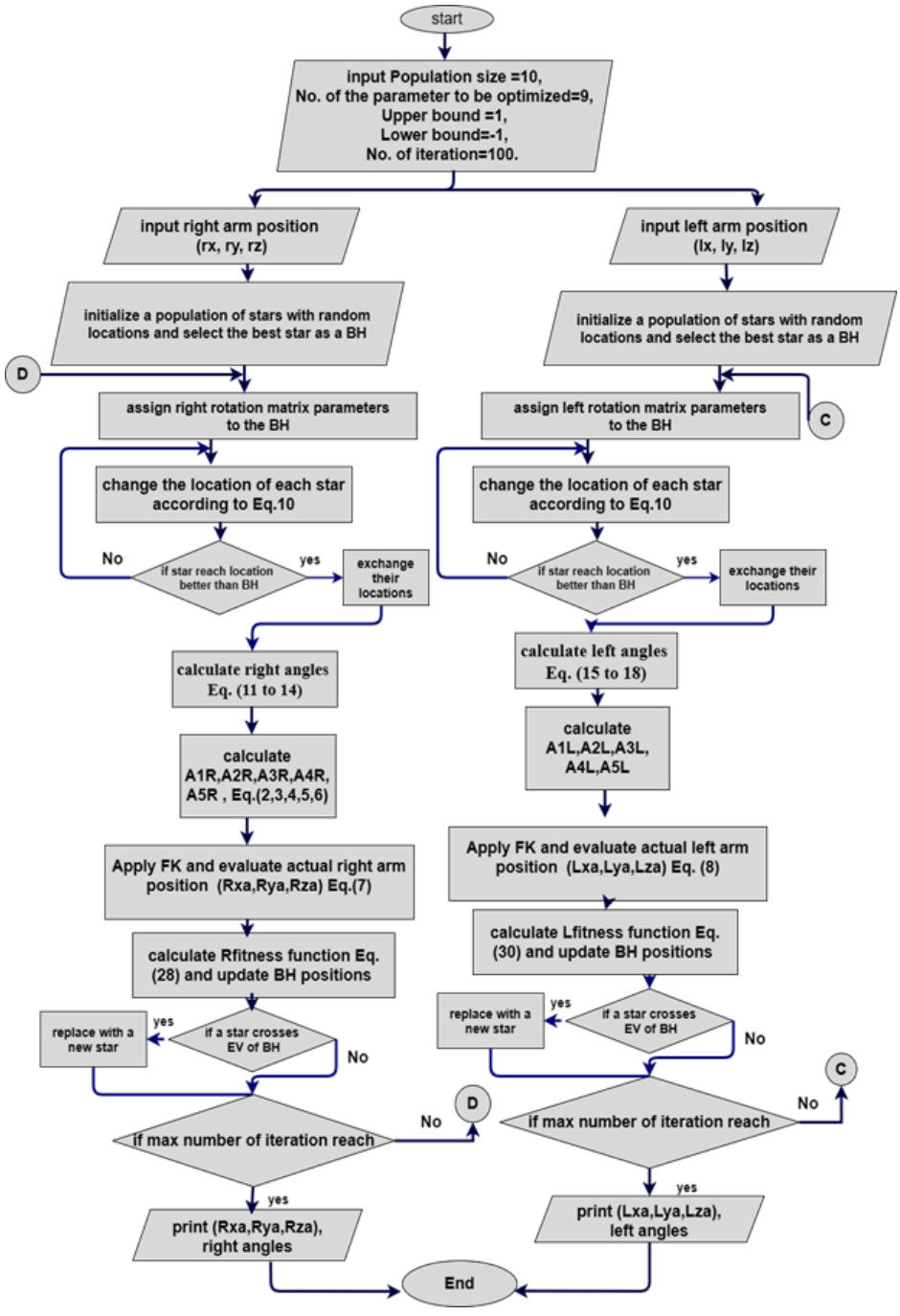

Figure 2: Flowchart for BHO algorithm

ISSN:2222-758X
e-ISSN:2789-7362

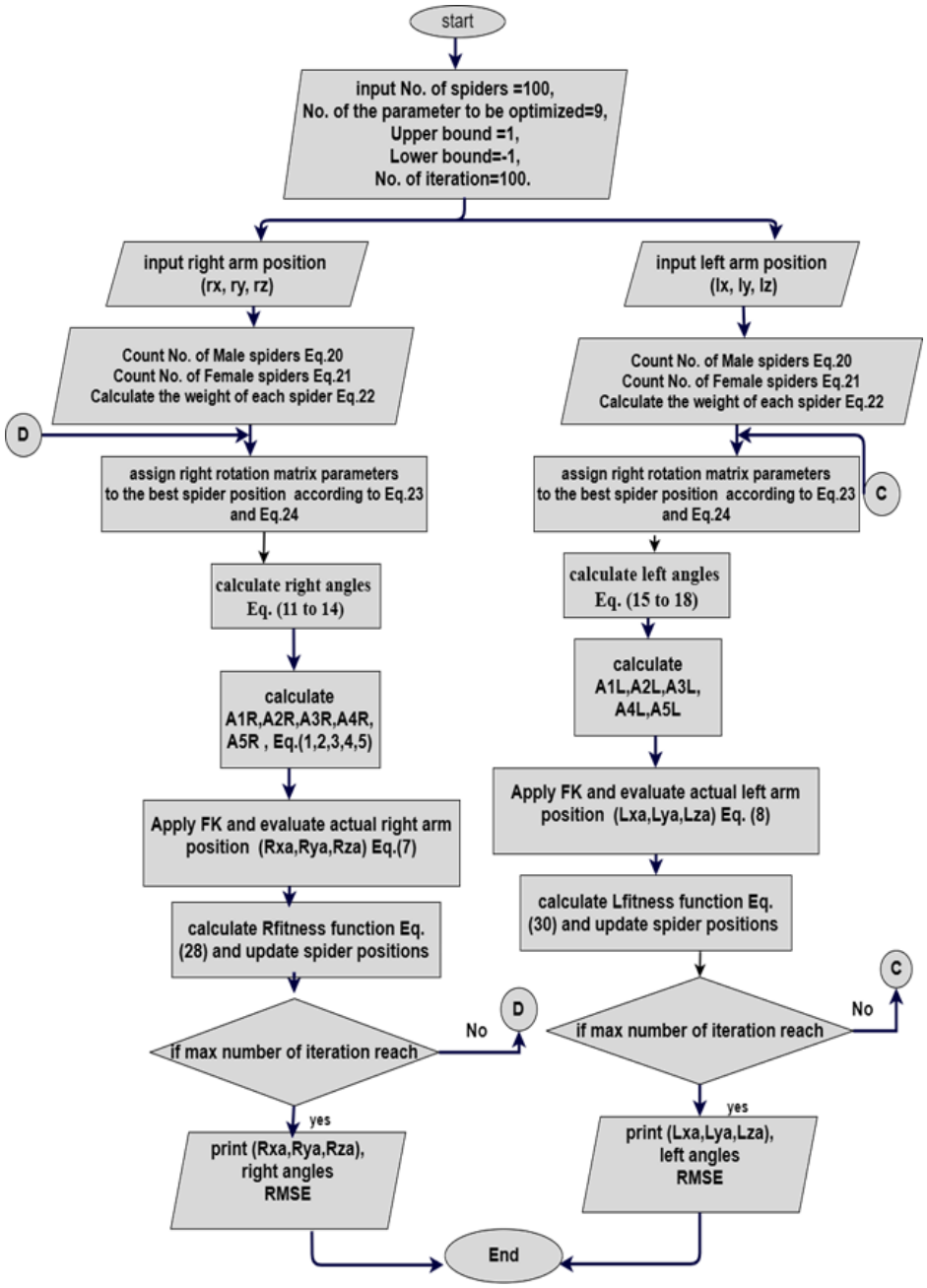

Figure 3: Flowchart for SSO algorithm

ISSN:2222-758X
e-ISSN:2789-7362

TABLE II
Setting of BHO, SSO, and PSO parameters

BHO		SSO		PSO	
Parameter	Value	Parameter	Value	Parameter	Value
Population size	10	Number of spiders	100	Population size	100
Dimension	9	Dimension	9	Dimension	9
Upper bound	1	Upper bound	1	Upper bound	1
Lower bound	-1	Lower bound	-1	Lower bound	-1
Number of Iteration	100	Number of Iteration	100	Number of Iteration	100

IV. LIMITATIONS OF HRAS AND SCENARIOS

This paper's objective is to test the performance of the proposed HRAs model and test the ability of HRAs to reach the desired position by right and left arms with minimum error and less time. Therefore, three optimization algorithms are proposed and comparisons are made between them to decide which one is better to solve the IK. Many positions are tested to check the actual position of each arm and calculate the CT and RMSE. Because of the limitation of this model, the workspace and operation area on which the arms move are specified within the constraint range listed in Table III.

TABLE III
The Constraints Range of HRA

Axis	Right arm		Left arm	
	Workspace (cm)	operation area (cm)	Workspace (cm)	operation area (cm)
X	-20 to 84	-20 to 20	20 to -84	-20 to 20
Y	0 to 64	0 to 40	0 to 64	0 to 40
Z	0 to -64	0 to -64	0 to -64	0 to -64

Six positions are desired in the operation and working areas to test the HRAs model. Fig. 4 describes these positions to be reached by right and left arms. Assuming that the HRAs model was placed at the point of origin and moving within the first and second quadrants.

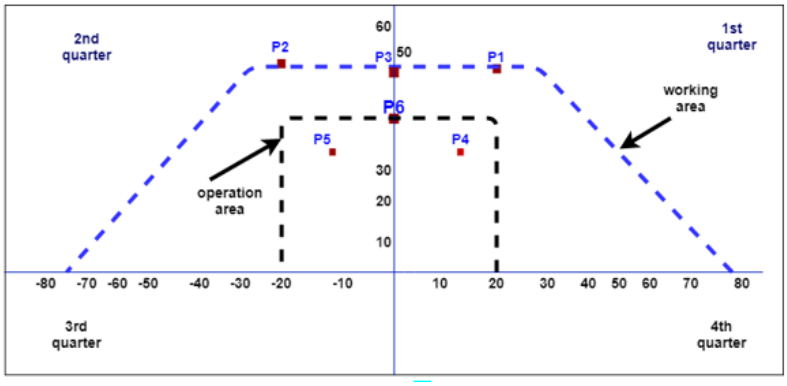

Figure 4: Preview of the desired positions in the working and operation area

Where the positions P5 and P4 are specified within the operation area. Position P6 is stated at the border of the operation area, while positions P1, P2, and P3 are selected at the border of the working area.

ISSN:2222-758X
e-ISSN:2789-7362

V. RESULTS

A comparison was made between the three optimization algorithms from point of view of CT and RMSE. Table IV lists a comparison result between optimal solutions using BHO, SSO, and PSO algorithms by evaluating RMSE and CT for a right arm. The same comparison is listed in Table V but for the left arm.

TABLE IV
Calculation Results for Right Arm

Case	Desired Position (cm)	BHO			SSO			PSO		
		Actual position (cm)	RMSE	CT (sec)	Actual position (cm)	RMSE	CT (sec)	Actual position (cm)	RMSE	CT (sec)
1	$\begin{bmatrix}20\\50\\0\end{bmatrix}$	$\begin{bmatrix}20\\50\\-2\times10^{-5}\end{bmatrix}$	1×10^{-4}	3.5000	$\begin{bmatrix}19.9999\\50.0001\\0.0001\end{bmatrix}$	0.0001	7.4827	$\begin{bmatrix}19.9904\\50.0001\\0.0001\end{bmatrix}$	0.0055	6.9845
2	$\begin{bmatrix}-20\\50\\0\end{bmatrix}$	$\begin{bmatrix}-20\\50\\-3\times10^{-4}\end{bmatrix}$	1×10^{-3}	3.2150	$\begin{bmatrix}-19.9996\\49.9008\\0.0122\end{bmatrix}$	0.0577	7.5312	$\begin{bmatrix}-19.9006\\50.1111\\0.0132\end{bmatrix}$	0.0864	6.8256
3	$\begin{bmatrix}0\\50\\-5\end{bmatrix}$	$\begin{bmatrix}3\times10^{-5}\\50\\-5\end{bmatrix}$	1×10^{-4}	3.0781	$\begin{bmatrix}0.0001\\50.9992\\-4.9981\end{bmatrix}$	0.0012	7.0231	$\begin{bmatrix}0.0002\\50.9998\\-4.9887\end{bmatrix}$	0.0065	6.5486
4	$\begin{bmatrix}0\\40\\-10\end{bmatrix}$	$\begin{bmatrix}-4\times10^{-8}\\40\\-10\end{bmatrix}$	2×10^{-7}	3.0156	$\begin{bmatrix}0.0001\\40\\-10.0000\end{bmatrix}$	0.00004	7.1265	$\begin{bmatrix}0.0001\\39.9999\\-10.0001\end{bmatrix}$	0.0001	6.0021
5	$\begin{bmatrix}15\\35\\-15\end{bmatrix}$	$\begin{bmatrix}15.00001\\35\\-15\end{bmatrix}$	5×10^{-5}	3.4156	$\begin{bmatrix}14.9999\\35.0001\\-15\end{bmatrix}$	0.00008	7.3521	$\begin{bmatrix}14.9998\\35.0001\\-15.0001\end{bmatrix}$	0.0001	6.3256
6	$\begin{bmatrix}-15\\35\\-15\end{bmatrix}$	$\begin{bmatrix}-15.00001\\35\\-15\end{bmatrix}$	5×10^{-5}	3.4557	$\begin{bmatrix}-14.9999\\35.0001\\-15\end{bmatrix}$	0.00008	6.4523	$\begin{bmatrix}-14.9998\\35.0001\\-15.0001\end{bmatrix}$	0.0001	6.2589

TABLE V
Calculation Results for Left Arm

Case	Desired Position (cm)	BHO			SSO			PSO		
		Actual position (cm)	RMSE	CT (sec)	Actual position (cm)	RMSE	CT (sec)	Actual position (cm)	RMSE	CT (sec)
1	$\begin{bmatrix}20\\50\\0\end{bmatrix}$	$\begin{bmatrix}20\\50\\-4\times10^{-4}\end{bmatrix}$	2×10^{-3}	3.2813	$\begin{bmatrix}19.9007\\50.0110\\0.0022\end{bmatrix}$	0. 0577	7.6521	$\begin{bmatrix}19.9006\\50.1111\\0.0132\end{bmatrix}$	0.0864	6.8205
2	$\begin{bmatrix}-20\\50\\0\end{bmatrix}$	$\begin{bmatrix}-20\\50\\-2\times10^{-5}\end{bmatrix}$	1×10^{-4}	3.4215	$\begin{bmatrix}-19.9997\\50.0001\\0.0000\end{bmatrix}$	0.0001	7.6251	$\begin{bmatrix}-19.9901\\50.0010\\0.0001\end{bmatrix}$	0.0058	6.7256
3	$\begin{bmatrix}0\\50\\-5\end{bmatrix}$	$\begin{bmatrix}2\times10^{-5}\\50\\-5\end{bmatrix}$	1×10^{-4}	3.0938	$\begin{bmatrix}0.0003\\49.9989\\-4.9958\end{bmatrix}$	0.0042	7.4523	$\begin{bmatrix}-0.0001\\49.9969\\-4.9888\end{bmatrix}$	0.0067	6.4452
4	$\begin{bmatrix}0\\40\\-10\end{bmatrix}$	$\begin{bmatrix}-4\times10^{-8}\\40\\-10\end{bmatrix}$	2×10^{-7}	3.0563	$\begin{bmatrix}0.0001\\40\\-10.0001\end{bmatrix}$	0.0000 4	7.0652	$\begin{bmatrix}0.0001\\39.9999\\-10.0001\end{bmatrix}$	0.0001	6.0005
5	$\begin{bmatrix}15\\35\\-15\end{bmatrix}$	$\begin{bmatrix}15.00001\\35.00001\\-15\end{bmatrix}$	5×10^{-5}	3.5412	$\begin{bmatrix}14.9999\\35.0001\\-15\end{bmatrix}$	0.0000 8	7.2568	$\begin{bmatrix}14.9999\\35.0001\\-15.0001\end{bmatrix}$	0.0001	6.5235
6	$\begin{bmatrix}-15\\35\\-15\end{bmatrix}$	$\begin{bmatrix}-15.00001\\35\\-15\end{bmatrix}$	5×10^{-5}	3.2564	$\begin{bmatrix}-14.9999\\35.0001\\-15\end{bmatrix}$	0.0000 8	7.1521	$\begin{bmatrix}-14.9999\\35.0001\\-15.0001\end{bmatrix}$	0.0001	6.4652

In those tables, the 1st, 2nd, and 3rd cases are the remotest area that the arms can reach, therefore, the RMSE and CT are greater than in other cases. As for the 1st case, it is selected in the 1st quadrant, and it is closer to the right arm. So, the RMSE and CT in this position are less than in the left arm. In contrast, in the 2nd case, the position is stated in the 2nd quarter nearby the left arm, so the RMSE and CT, in this case, are better for the left arm. The worst RMSE and CT values appeared in those cases. The third position was taken in the middle of the distance between the arms, exactly on

ISSN:2222-758X
e-ISSN:2789-7362

the Y-axis. The 5th and 6th cases are taking within the working area. The area in these cases is most used by both arms. In these two cases, the values of RMSE and CT are better than the first three cases, because these positions are nearer to the arms than in the first three cases. The 4th case is stated at the border of the working area, and it is the best case. The minimum values of RMSE and CT are calculated in this case using BHO algorithm. It has the best RMSE which is 2×10^{-7} for both arms and less CT which are 3.0156 and 3.0563 seconds for right and left arms respectively. Calculation results in Tables IV and V showed that the BHO algorithm is more accurate than the other optimization algorithms for all six cases. The difference in RMSE from one position to another is appeared because of non-linearity in trigonometric functions. Moreover, through the results, we notice that the SSO algorithm was a case in the between of the two other optimization algorithms in the calculation of RMSE but PSO is better than SSO in CT. GUI is designed to test and simulate the emotional characteristics of the HRAs model based on BHO. Two cases are used to simulate the HRAs model-based BHO algorithm. The fourth case from the above tables is simulated at the border of the operation area as shown in Fig. 5. Also, the sixth case is simulated inside the operation area as shown in Fig. 6.

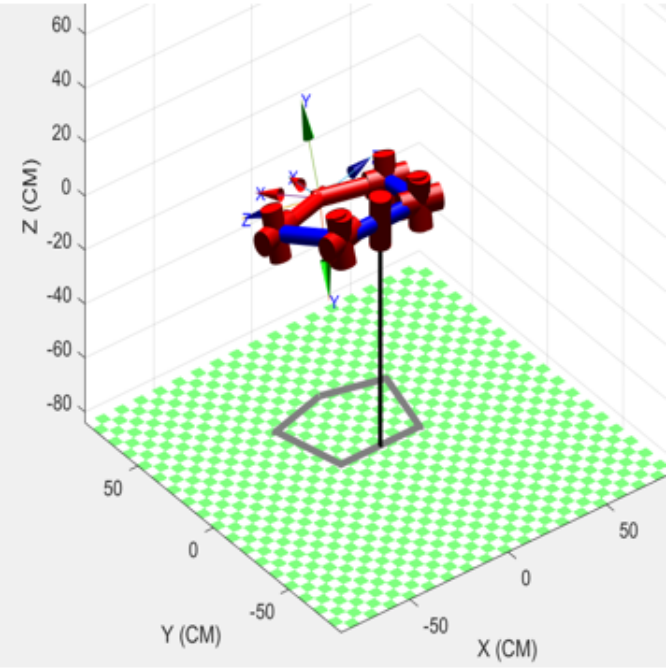

Figure 5: Fourth case GUI simulation based BHO

ISSN:2222-758X
e-ISSN:2789-7362

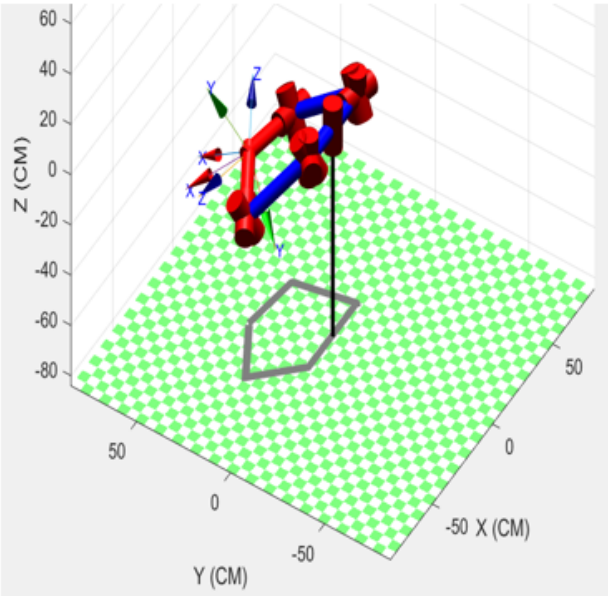

Figure 6: Sixth case GUI simulation based

VI. Conclusion

In this paper, a solution for the IK of the HRAs model is proposed to improve the accuracy and minimize the RMSE and CT for both arms. HRAs model is designed based on the DH parameter method to define the kinematics problem. Three optimization algorithms; BHO, SSO, and PSO algorithms were designed to solve the IK problem to obtain the required angles and desired position with minimum RMSE and less CT for right and left arms. The HRAs model is tested by several desired positions. The first two cases are the worst. They are chosen at the border of the working area, which are the farthest positions that the arms can reach. While the best is the fourth case which is taken in the working area. In all six cases, calculations and results showed that; the proposed BHO has better performance and higher accuracy than SSO and PSO and less CT. Also, the SSO algorithm showed that it was better than the PSO algorithm in RMSE. We got the largest RMSE which is 0.0864 in the first two cases using the PSO algorithm for both arms. But in the 4th case, we got the lowest possible error, which is 2×10^{-7} , this error happened because of the non-linearity of trigonometric functions. In all six desired positions, the BHO showed that it was better than the other two optimization algorithms in terms of CT in which the less CT is calculated using the BHO algorithm which is 3.0156 seconds for the right arm.

ISSN:2222-758X
e-ISSN:2789-7362

REFERENCES

[1] J. Craig, "Introduction to Robotics, Mechanics and Control" , 4th ed. Pearson, London, 2017.
[2] C. Caraveo, F. Valdez and O. Castillo, "A New Bio-Inspired Optimization Algorithm Based on the Self-defense Mechanism of Plants in Nature" , Springer International Publishing , 2019.
[3] S. B. Niku, "Kinematics of Robots: Position Analysis" , in Introduction to robotics: analysis, control, applic-ations, Edited, Linda Ratts, John Wiley and Sons, Vol. 2, pp. 33-113, 2010.
[4] A. A. Al-Hamadani, M. Z. Al-Faiz, and S. Member, "Inverse Kinematic Based Brain Computer Interface to Control Humanoid Robotic Arm" , Int. J. Mech. Mechatronics Eng. IJMME-IJENS, Vol. 20, No. 01, pp. 15-24, 2020.
[5] M. Z. Al-Faiz and M. S. Saleh, "Inverse Kinematics Analysis for Manipulator Robot with Wrist Offset Based On the Closed-Form Algorithm" , Int. J. Robot. Autom. , Vol. 2, No. 4, pp. 256-264, 2011.
[6] M. Z. Al-Faiz, A. H.Miry, and A. A .Ali, "Simulation of Digital Control of Human Arm Based PSO Algorithm in Virtual Reality" , Journal of Engineering and Development, Vol. 16, No. 3, Sep. , 2012.
[7] N. Rokbani and A. M. Alimi, "Inverse Kinematics Using Particle Swarm Optimization, A Statistical Analysis" , International Conference On Design and Manufactuing, Vol. 64, pp. 1602- 1611, 2013.
[8] R. Javidan and H. Khuban, "Optimal Non-Integer PID Controller for A Class of Nonlinear Systems: Multi-Objective Modified Black Hole Optimization Algorithm" , Neural Computer & Application, 2018.
[9] A. Haneen, A. Noraziah, A. AbdulRahman and S. Sinan, "An Enhanced Version of Black Hole Algorithm Via Levy Flight for Optimization and Data Clustering Problems" , IEEE Access, 2019.
[10] H.I. Ali, M.A. Hadi, "Optimal Nonlinear Controller Design for Different Classes of Nonlinear Systems Using Black Hole Optimization Method" , Arab Journal of Science Engineering, Vol. 45, pp. 7033-7053, 2020.
[11] A. Hatamlou, "A New Heuristic Optimization Approach for Data Clustering" , Information Science, pp. 175-184, 2013.
[12] H. M. Zawbaa, E. Emary and A. E. Hassanien, "A Wrapper approach for Feature Selection Based on Swarm Optimization Algorithm Inspired from the Behavior of Social-Spider" , Seventh International Conference of Soft Computing and Pattern Recognition, pp. 25-30, 2015.
[13] Z. Yongquan, Y. Zhou, Q. Luo, and M. Abdel-Basset, "A Simplex Method-Based Social Spider Optimization Algorithm for Clustering Analysis" , Engineering Applications of Artificial Intelligence , pp. 67-82, 2017.